X-ray reflectivity fine structure from homogeneous materials in the hard-energy range

1995 J. Phys.: Condens. Matter 7 3779

(http://iopscience.iop.org/0953-8984/7/19/012)

J. Phys.: Condens. Matter 7 (1995) 3779–3787. Printed in the UK

X-ray reflectivity fine structure from homogeneous materials in the hard-energy range

P Borthen and H-H Strehblow

Institut für Physikalische Chemie und Elektrochemie, Heinrich-Heine-Universität Düsseldorf, 40225 Düsseldorf, Germany

Received 7 December 1994, in final form 21 February 1995

Abstract. To a good approximation, the x-ray reflectivity fine structure from homogeneous materials was found to be, in the hard-energy range, a linear superposition of the fine structures of the real and imaginary parts of the refractive index. As a consequence, a simple formula for the extraction of the absorption fine structure (EXAFS) from the reflectivity data is given. For a certain glancing angle, the Kramers–Kronig transform of the reflectivity fine structure is, to a constant factor, approximately equal to EXAFS. The magnitudes of the Fourier transform of the reflectivity fine structure and of EXAFS have for all glancing angles approximately the same shape.

1. Introduction

The increasing availability of intense x-ray sources in recent years has stimulated a growth in popularity of grazing incidence methods. Due to the low penetration depth of about a few nanometres, these methods are well suited for studies of surface layers and near-surface regions. One of these methods is the extended x-ray absorption fine structure spectroscopy (EXAFS).

As stated firstly by Barchewitz *et al* [1], x-ray reflectivity spectra recorded in the vicinity of an absorption edge exhibit a fine structure similar to the EXAFS oscillations. The more detailed investigations of Martens *et al* [2] showed that compared with the absorption fine structure, this fine structure is modified due to the influence of the real part of the refractive index. Thus, the measured reflectivity spectra must be corrected in some way to obtain the true absorption fine structure. Heald *et al* developed a correction method based on the knowledge of the smooth part of the refractive index for the system of interest [3]. An iterative procedure combined with the Kramers–Kronig transform of the oscillatory part of the reflectivity was used by Poumellec *et al* [4]. For measurements performed at glancing angles small compared to the critical angle, an approximative relation between the x-ray reflectivity and EXAFS was given [5].

Some of the grazing incidence EXAFS measurements reported in the literature were performed by recording the fluorescence radiation. However, we restrict our considerations to the reflected intensity: it has the advantage of being simply modelled by the Fresnel equations—also for layer systems—without problems caused by the radiation efficiency and the self-absorption of the fluorescent radiation. In this paper, we report on the x-ray reflectivity fine structure (XRFS) for homogeneous materials in the hard-energy range, its relation to the fine structures of the refractive indices and the consequences for the data analysis.

0953-8984/95/193779+09$19.50

2. X-ray reflectivity

If the surface roughness can be neglected, the energy-dependent reflectivity of a given medium can be fully characterized by its index of refraction $n(E) = 1 - \delta(E) - i\beta(E)$ [6]. Reflectivity spectra $R(E)$ recorded in the vicinity of an absorption edge at angles well below the critical angle $\Theta_c = (2\delta)^{1/2}$ differ substantially from those recorded above Θ_c [2]. Aside from the absolute value of the reflectivity and the overall shape of the curves, the fine structure in the reflectivity above the absorption-edge energy also changes significantly.

As an example, reflectivity spectra recorded at 3.3 mrad and 7.7 mrad in the vicinity of the Ni K edge from a nickel specimen are shown in figures 1(*a*) and (*b*), respectively. The critical angle for nickel is about 6.6 mrad (0.38 degrees) at 8200 eV. The specimen was a 5 cm long and 0.125 mm thick metal foil (99.98%, Goodfellow) stuck, under pressure, onto a float glass substrate and subsequently polished with a 40 nm SiO_2 suspension. Due to the polishing procedure, the uncertainty of the glancing angle, caused by the surface curvature, was about 0.1 mrad (0.006 degrees). The spectra were recorded at the HASYLAB RÖMO 2 station (DESY, Germany) immediately after the polishing.

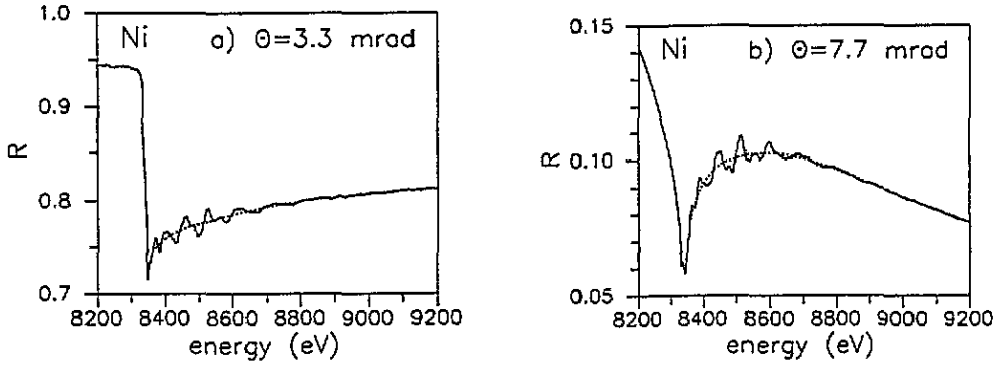

Figure 1. X-ray reflectivity spectra for a polished nickel specimen recorded at glancing angles; (*a*) below and (*b*) above the critical angle, respectively.

Above the absorption edge, the x-ray reflectivity, R, can be split into a smooth part, R_0, and an oscillatory part, ΔR, (the dashed and the solid lines in figures 1(*a*) and (*b*), respectively) with $R = R_0 + \Delta R$. For an angle of incidence Θ and a refracted angle Θ', the Fresnel reflectivity is given by

$$R = \left|\frac{\Theta - \Theta'}{\Theta + \Theta'}\right|^2 \tag{1}$$

where $\Theta' = u + iv$ and

$$\begin{aligned} u^2 &= \tfrac{1}{2}\left(\sqrt{(\Theta^2 - 2\delta)^2 + 4\beta^2} + (\Theta^2 - 2\delta)\right) \\ v^2 &= \tfrac{1}{2}\left(\sqrt{(\Theta^2 - 2\delta)^2 + 4\beta^2} - (\Theta^2 - 2\delta)\right). \end{aligned} \tag{2}$$

It is evident from equations (1) and (2) that the x-ray reflectivity depends in a complicated manner on δ and β. Therefore, δ as well as β have to be known with good accuracy as

functions of energy in order to calculate the reflectivity $R(E)$ in the vicinity of absorption edges.

Due to the relation $\beta = \mu\lambda/4\pi$, where λ is the wavelength, an absorption spectrum $\mu(E)$ is the most convenient source for $\beta(E)$-values. The $\delta(E)$ values can be calculated from the $\beta(E)$ using the Kramers–Kronig transform if $\beta(E)$ is known over a wide enough energy range. For calculations near the K edge of a given material, the knowledge of $\beta(E)$ between the L_I edge and about 5–10 times the K-edge energy is usually sufficient. We denote the Kramers–Kronig relation that transforms the $\beta(E)$ values to the $\delta(E)$ values by KK: $\delta = \mathrm{KK}(\beta)$. The inverse transform is then given by $\beta = \mathrm{KK}^{-1}(\delta)$. Above the absorption edge energy $\beta(E)$ can be split into a smooth (β_0) and an oscillatory part ($\Delta\beta$): $\beta = \beta_0 + \Delta\beta$. due to the linearity of the Kramers–Kronig transform we can write: $\mathrm{KK}(\beta) = \mathrm{KK}(\beta_0) + \mathrm{KK}(\Delta\beta)$. The smooth part of δ can be defined as: $\delta_0 = \mathrm{KK}(\beta_0)$ and the oscillatory part as: $\Delta\delta = \mathrm{KK}(\Delta\beta)$. This can be justified by calculating $\Delta\delta_1 = \mathrm{KK}(\beta) - \mathrm{KK}(\beta_0)$ and $\Delta\delta_2 = \mathrm{KK}(\Delta\beta)$ separately, where $\Delta\delta_1 = \Delta\delta_2$. Therefore, the functions $\Delta\delta(E)$ and $\Delta\beta(E)$ form a Kramers–Kronig transform pair. The $\beta(E)$, $\delta(E)$, $\Delta\beta(E)$ and $\Delta\delta(E)$ values for nickel are shown in figures 2(a) and (b), respectively.

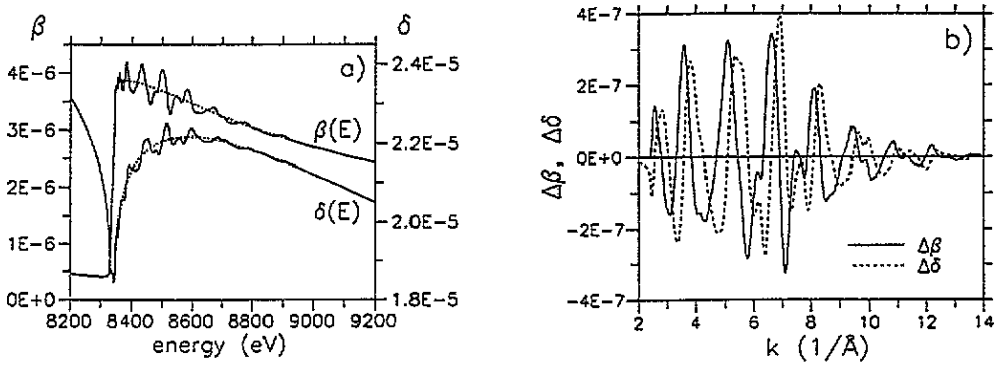

Figure 2. (a) δ and β as functions of energy. The $\beta(E)$ values were obtained from a transmission EXAFS spectrum with a nickel foil. $\delta(E)$ is the Kramers–Kronig transform of $\beta(E)$. Dashed: smooth parts of δ and β (δ_0 and β_0) above the absorption edge energy. (b) Fine structures in δ: $\Delta\delta = \delta - \delta_0$ and β: $\Delta\beta = \beta - \beta_0$.

The calculation of $\Delta R(E)$ is straightforward, if δ and β values are known: $\Delta R = R(\delta, \beta) - R(\delta_0, \beta_0)$, where R is given by equation (1). However, such a simple formula cannot be given in those cases, where only $\delta_0(E)$ and $\beta_0(E)$ are known and ΔR as a function of $\Delta\delta$ and $\Delta\beta$ has to be found.

In the first order, ΔR can be written as

$$\Delta R \approx \Delta R_{\text{approx.}} = \frac{\partial R}{\partial \delta}\Delta\delta + \frac{\partial R}{\partial \beta}\Delta\beta \tag{3}$$

where the partial derivatives are calculated for $\delta = \delta_0$ and $\beta = \beta_0$. However, comparisons of calculated exact reflectivities with those given by equation (3) show that this approximation is valid only for glancing angles significantly below Θ_c. As shown in figure 3, both partial derivatives, as well as their ratio, have a strong energy dependence.

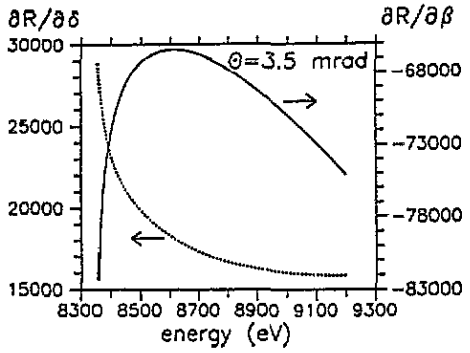

Figure 3. Partial derivatives of reflectivity R for $\delta = \delta_0$ and $\beta = \beta_0$ as functions of energy calculated for $\Theta = 3.5$ mrad using the Fresnel equation.

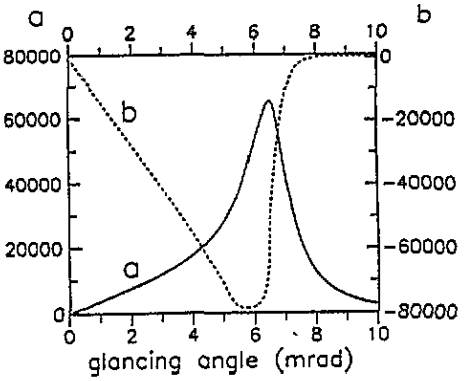

Figure 4. Weighting factors a and b obtained with calculated nickel reflectivity fine structure.

In contrast to equation (3), a linear *ansatz* for $\Delta R(E)$, with energy independent weighting factors a and b, yields a significantly better approximation

$$\Delta R_{\text{approx.}} = a\,\Delta\delta + b\,\Delta\beta. \tag{4}$$

For a given substance, the numbers a and b depend only on the glancing angle. The approximation given by equation (4) is applicable for glancing angles below as well as above the critical angle. The determination of a and b for a given substance can be achieved according to the following procedure

(i) recording of the EXAFS spectrum in transmission from a model compound,

(ii) determination of $\beta(E)$ from this spectrum and calculation of $\delta(E)$ values using the Kramers–Kronig transform,

(iii) calculation of $R(E)$ and $\Delta R(E)$ with equation (1) and

(iv) linear fit of the $\Delta R(E)$ function with the $\Delta\delta$ and $\Delta\beta$ values obtained in step (ii).

Figure 4 shows the a and b values as functions of Θ obtained for the reflectivity fine structures calculated with the data from figures 2(a) and (b). Each pair of numbers a and b is the result of a separate run of the fit procedure using the same $\Delta\beta(E)$ values and the corresponding $\Delta\delta(E)$ values.

The relative error of the approximation (4) for a spectrum with N data points can be defined as

$$\text{fit error} = \sum_{i=1}^{N}(\Delta R^{(i)} - \Delta R^{(i)}_{\text{approx.}})^2 \Big/ \sum_{i=1}^{N}(\Delta R^{(i)})^2 \tag{5}$$

where i is the number of the data point and ΔR is the true reflectivity fine structure. The fit errors as a function of the glancing angle for the calculated nickel reflectivity spectra are shown in figure 5. The error has its maximum value of about 0.12 in the vicinity of Θ_c, but is significantly smaller for all other angles. Figure 6 shows ΔR and $\Delta R_{\text{approx.}} = a\Delta\delta + b\Delta\beta$ for the angle with the maximum fit error. The approximation is acceptable also in this worst case.

The ratio b/a describes the relative $\Delta\beta$ and $\Delta\delta$ contribution to ΔR. As can be seen in figure 7, this ratio changes significantly with Θ. Whereas the $\Delta\delta$ contribution is greater

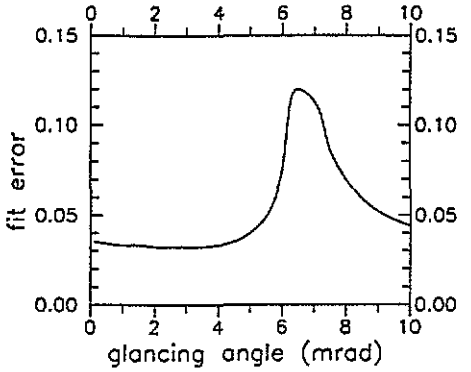

Figure 5. Fit errors as defined by equation (5) for data in figure 4.

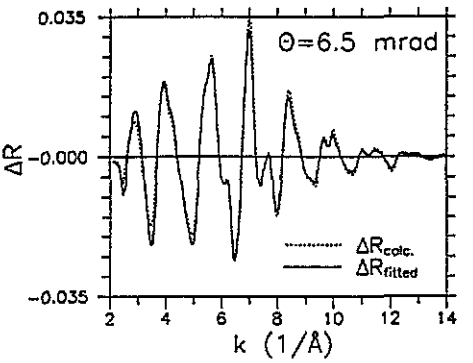

Figure 6. Calculated nickel reflectivity fine structure ΔR (dashed) and the result of a linear fit using $\Delta\delta$ and $\Delta\beta$ values (solid).

than zero for all angles, that of $\Delta\beta$ vanishes at $\Theta^* \simeq 7.9$ mrad. Therefore, the reflectivity recorded at Θ^* has—within this approximation—a fine structure which is proportional to $\Delta\delta$ with a fit error of about 0.07. The inverse Kramers–Kronig transform then yields, to a constant factor, $\Delta\beta$. Θ^* is the only angle at which the reflectivity fine structure reveals that of the absorption coefficient.

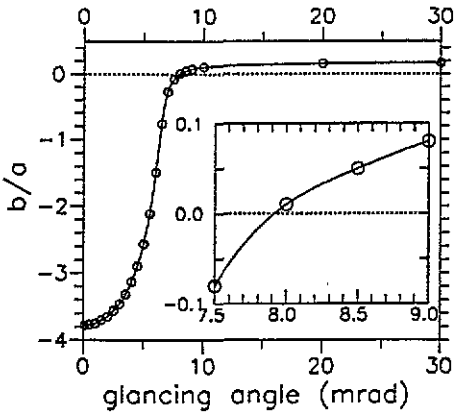

Figure 7. Approximative relative $\Delta\beta$ and $\Delta\delta$ contribution (b/a) for calculated nickel ΔR data at glancing angles between 0 and 30 mrad. b/a vanishes at $\Theta \simeq 7.9$ mrad; at this angle ΔR is proportional exclusively to $\Delta\delta$.

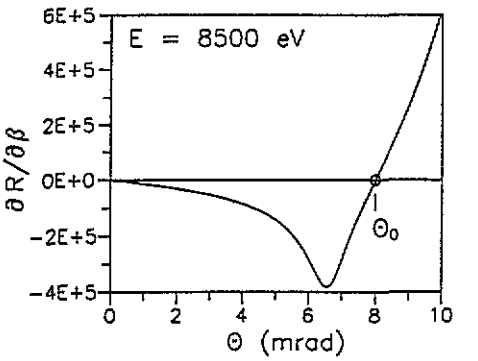

Figure 8. $\partial R/\partial\beta$ for $\beta = \beta_0$ as a function of glancing angle at a fixed energy value. In contrast to $\partial R/\partial\delta$, $\partial R/\partial\beta$ vanishes at a specific glancing angle Θ_0.

Though the approximation given by equation (3) is applicable only for $\Theta < \Theta_c$, an approximate value for Θ^* can be obtained from the properties of the partial derivative $\partial R/\partial\beta$ as a function of energy and as a function of Θ. As shown in figure 8, the partial derivative calculated for $\delta = \delta_0$ and $\beta = \beta_0$ as a function of Θ for a fixed energy value vanishes at a certain angle Θ_0. In contrast to that, $\partial R/\partial\delta$ is positive for all $\Theta > 0$. In

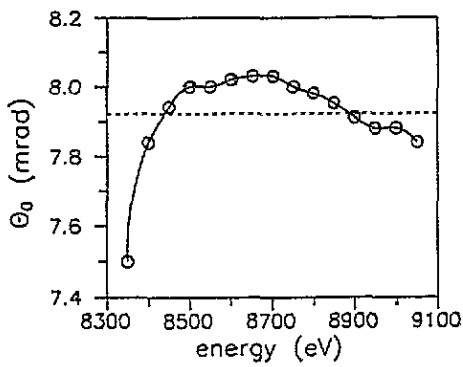

Figure 9. Θ_0 for calculated nickel $\partial R/\partial\beta$ data as a function of energy. The mean value of Θ_0 in the EXAFS energy range (dashed line) is 7.9 mrad.

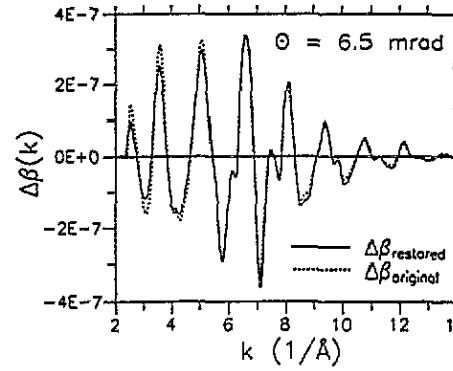

Figure 10. Original $\Delta\beta(E)$ function and the values restored from the calculated nickel reflectivity fine structure for $\Theta = 6.5$ mrad using equation (9).

figure 9, Θ_0 values as a function of energy are shown. The value of Θ_0 scatters in the Ni-EXAFS energy range about a mean value $\Theta_{0,\mathrm{mean}}$ with $\Theta_{0,\mathrm{mean}} \simeq \Theta^*$.

The relation $\Delta R \simeq a\Delta\delta + b\Delta\beta$ can be used for the calculation of the Fourier transform (FT) of $\Delta R(k)$, where k is the wavevector. We note first, that $\mathrm{FT}(\Delta\beta)$ is a complex valued function in the distance (r) space. Then, with $\Delta\delta = \mathrm{KK}(\Delta\beta)$ we obtain [7]

$$\mathrm{FT}(\Delta\delta) = \begin{cases} \mathrm{i}\,\mathrm{FT}(\Delta\beta) & r \geqslant 0 \\ -\mathrm{i}\,\mathrm{FT}(\Delta\beta) & r < 0. \end{cases} \tag{6}$$

From equations (4) and (6), then follows

$$|\mathrm{FT}(\Delta R)| \approx (a^2 + b^2)^{1/2} |\mathrm{FT}(\Delta\beta)|. \tag{7}$$

Due to the angle dependence of a and b (as shown in figure 4 and according to equation (7)), the magnitude of the Fourier transform of ΔR depends strongly on the glancing angle. Such angle dependence is also experimentally observed. Although the magnitude of $|\mathrm{FT}(\Delta R)|$ considerably varies with the angle, its shape is for all angles approximately the same as that of $|\mathrm{FT}(\Delta\beta)|$. Therefore, for a homogeneous specimen the magnitude of the XRFS Fourier transform is, to a constant factor, approximately equal to that of the specimen EXAFS—independent of the glancing angle at which the spectrum was recorded. If, on the other hand, the observed shape of $|\mathrm{FT}(\Delta R)|$ does change with the glancing angle, then there is a structural inhomogeneity within the specimen x-ray penetration depth. The Fourier transform of ΔR is therefore a valuable tool in connection with the x-ray reflectivity fine structure spectroscopy.

3. EXAFS extraction

With the approximation given by equation (4), $\Delta\beta(E)$ can be extracted from the reflectivity data if the weighting factors a and b are known. We note first, as a consequence of the properties of the Hilbert transform, that the Kramers–Kronig transform of $\Delta\delta$ is given by $\mathrm{KK}(\Delta\delta) = -\Delta\beta$.

If the Kramers–Kronig transform is performed for both sides of equation (4), then

$$\mathrm{KK}(\Delta R) \approx b\,\Delta\delta - a\,\Delta\beta. \tag{8}$$

From equations (4) and (8) we then obtain

$$\Delta\beta(E) \approx \frac{1}{a^2+b^2}(b\Delta R(E) - a\mathrm{KK}(\Delta R(E))). \tag{9}$$

Equation (9) can be applied for the extraction of the EXAFS from the measured XRFS if

(i) the weighting factors a and b were obtained with a model compound data or, alternatively, using results of a numerical simulation and

(ii) the specimen is homogeneous in the range of the x-ray penetration depth.

In figure 10, the original $\Delta\beta(E)$ data are compared with those calculated with equation (9). The reflectivity fine structure for this comparison was calculated with nickel data from figures 2(a) and (b) for $\Theta = 6.5$ mrad. In figure 11, the magnitudes of both Fourier transforms are depicted. The agreement between the original and the extracted $\Delta\beta$ data is reasonably good despite the fact, that the fit error has a maximum at $\Theta = 6.5$ mrad.

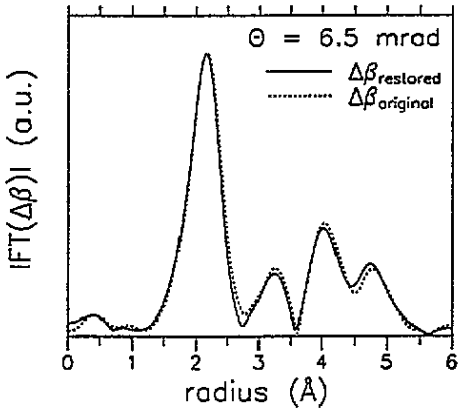

Figure 11. Magnitudes of the Fourier transforms for the original and the restored $\Delta\beta(E)$ data.

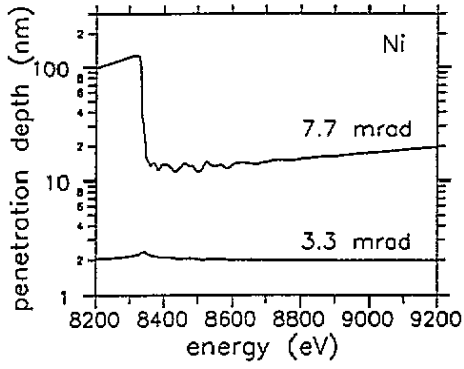

Figure 12. X-ray penetration depths for nickel for the glancing angles $\Theta = 3.3$ mrad and $\Theta = 7.7$ mrad, respectively, as a function of energy.

In this context, it can be noted that oscillatory functions like $\Delta\beta(k)$ and $\Delta R(k)$ can be very fastly Kramers–Kronig transformed using the fast Fourier transform (FFT). With $\mathrm{FT}(\delta)$ from equation (6), the Kramers–Kronig transform of $\Delta\beta$ is given by $\mathrm{KK}(\Delta\beta) = \mathrm{FT}^{-1}[\mathrm{FT}(\Delta\delta)]$.

4. Example

The a and b values obtained with the simulated XRFS data can be applied to the experimental reflectivity data shown in figures 1(a) and (b). Although the penetration depths for $\Theta = 3.3$ mrad and $\Theta = 7.7$ mrad differ strongly, they vary only moderately at a fixed

angle as functions of the energy in the EXAFS region above the absorption edge (figure 12). It is well known, that metals surfaces are spontaneously covered with a thin oxide layer. We estimated its thickness in the case of the nickel specimen to about 0.5 nm. Therefore, due to the low penetration depth of x-rays of about 2.5 nm at 3.3 mrad the reflectivity is slightly influenced by the oxide layer at that angle with almost unchanged EXAFS structure (figure 13(*a*)). At 7.7 mrad, the XRFS transformed with equation (9) is very similar to the fine structure in β calculated with data obtained from a metal foil in transmission (figure 13(*b*)).

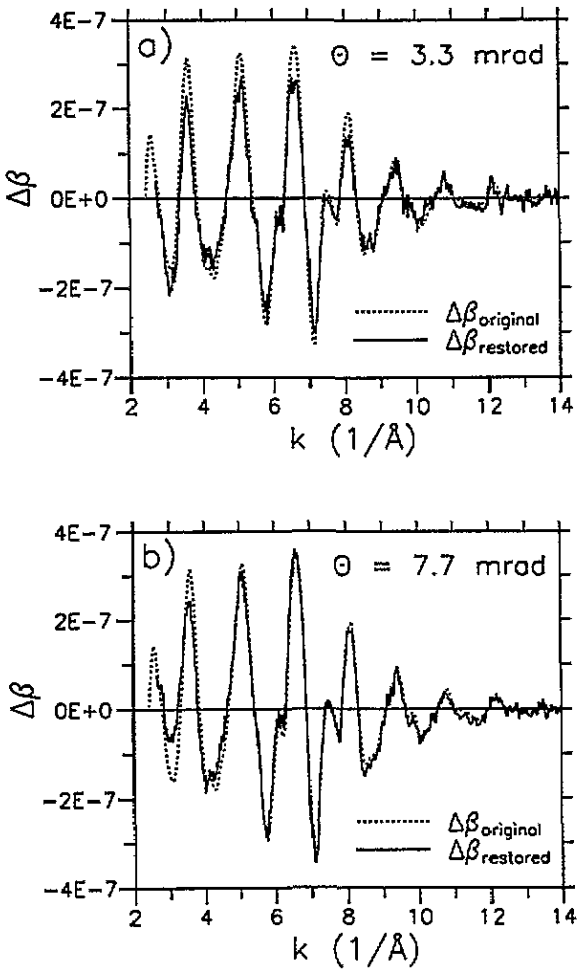

Figure 13. Original $\Delta\beta(E)$ function and the values restored from the measured nickel reflectivity fine structure for $\Theta = 3.3$ mrad (*a*) and $\Theta = 7.7$ mrad (*b*) using equation (9).

5. Conclusions

The x-ray reflectivity fine structure for homogeneous materials can be, to a good approximation, described as a linear superposition of the fine structures in the real and the

imaginary part of the refractive index $\Delta\delta$ and $\Delta\beta$, respectively. For a specific angle above the critical angle, the reflection fine structure is proportional to $\Delta\delta$ only, the Kramers–Kronig transform of which is, to a constant factor, $\Delta\beta$. At all other angles, $\Delta\beta$ can be obtained from the XRFS using a simple formula. For all glancing angles $|\mathrm{FT}(\Delta R)|$ is approximately proportional to $|\mathrm{FT}(\Delta\beta)|$.

Acknowledgments

We would like to thank J-M Abels and D Hecht for their help with the experiments. We also thank D Hecht for critical reading of the manuscript. This work was supported by the BMFT under project No 055 FF AB 0.

References

[1] Barchewitz R, Cremonese-Visicato M and Onori G 1978 *J. Phys. C: Solid State Phys.* **11** 4439
[2] Martens G and Rabe P 1981 *J. Phys. C: Solid State Phys.* **14** 1523
[3] Heald S M, Chen H and Tranquada J M 1988 *Phys. Rev.* B **38** 1016
[4] Poumellec B, Cortes R, Lagnel F and Tourillon G 1989 *Physica* B **158** 282
[5] Bosio L, Cortes R, Defrain A and Froment M 1984 *J. Electroanal. Chem.* **180** 265
[6] James R W 1958 *The Optical Principles of the Diffraction of X-rays* (London: Bell)
[7] Papoulis A 1977 *Signal Analysis* (New York: McGraw-Hill)